Cohesive Zone Analysis for Interface Debonding in AA6061/Titanium Nitride Nanoparticulate Metal Matrix Composites

[1]S. Sundara Rajan and A. Chennakesava Reddy[2]

[1]Scientist-F, Defence Research and Development Organisation, Hyderabad, India
[2]Assistant Professor, Department of Mechanical Engineering, MJ College of Engineering and Technology, Hyderabad, India
dr_acreddy@yahoo.com

Abstract: *Diamond array unit cell/2-D rectangular particulate RVE models were used to estimate interface debonding using cohesive zone analysis. The particulate metal matrix composites are titanium nitride/AA6061 alloy at different volume fractions of titanium nitride. Interface debonding was observed in all the composites.*

Keywords: AA6061, *titanium nitride, rectangular particulate, RVE model, finite element analysis, interface debonding.*

1. INTRODUCTION

Linear Elastic Fracture Mechanics (LEFM) is used for dealing with crack propagation, but requires knowledge of an already existing crack [1]. Cohesive zone modeling (CZM) offers no initial crack, but still relies on well known properties such as critical energy release rates. The Cohesive zone concept was proposed by Barenblatt [2]. The cohesive zone model divides a crack into two parts. The cohesive zone is idealized as two cohesive surfaces which are held together by tractions.

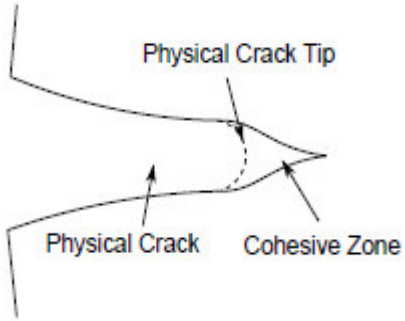

Figure 1: Distinction of the two different zones in the crack.

The tractions [2-14] in the cohesive zone are related to the relative displacements of the cohesive surfaces through a constitutive law. A physical crack extension occurs when the relative displacements in the cohesive zone reach a critical value. A sketch of a cohesive zone with tractions, T, as a function of separation distance, Δ is shown on figure 2.

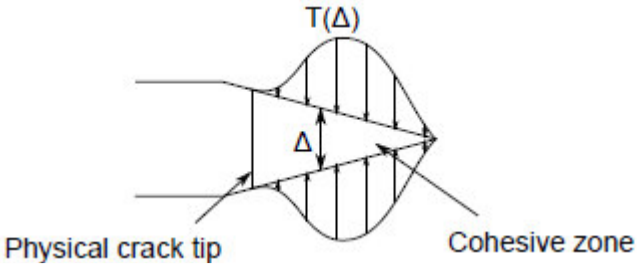

Figure 2: A cohesive zone with tractions, T, as a function of separation distance.

In the present research, the cohesive zone analysis was carried out to predict interface debonding in the AA6061/titanium nitride nanoparticulate-reinforced composites. In the analysis, the two cases of interfacial debonding and particulate fracture were studied. Representative volume elements (RVEs) models were taken from the periodic 2-D rectangular particulates in a diamond array distribution.

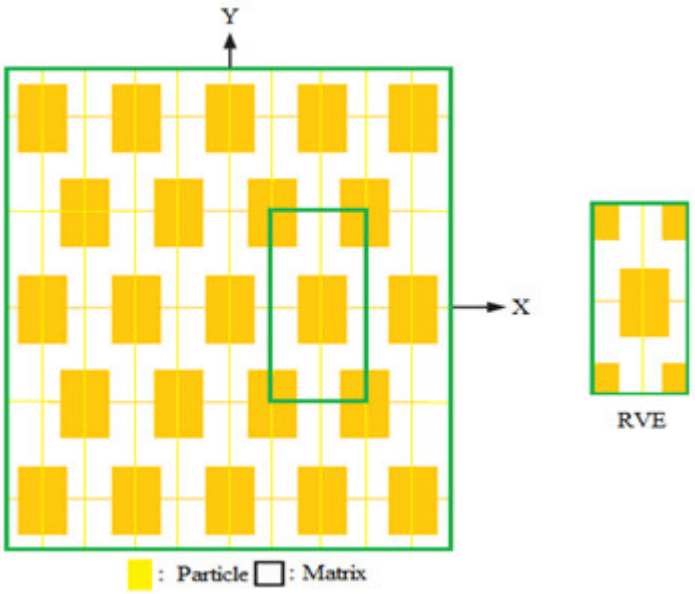

Figure 3: The RVE model: (a) particle distribution and (b) RVE scheme.

2. MATERIALS AND METHODS

The volume fractions of titanium nitride used in the present work were 10%, 20%, and 30% TiN. The matrix material was AA6061 alloy. The periodic model for the representative volume element (RVE) scheme was constructed from 2-D rectangular particulates in a diamond array particulate distribution (figure 3). PLANE183 element was used for the matrix and the nanoparticulate. The cohesive zone can be incorporated in the continuum formulation by applying the cohesive tractions as boundary conditions. When the discretization is set up, two types of elements are required. One element is a continuum type element and the other a CZM type element. The Newton-Raphson Method (NRM) is used as it supports the concept of a tangent stiffness matrix. The cohesive element is implemented as a linear element with four nodes. The isoparametric formulation is chosen for the element, meaning that shape and displacements are interpolated by the same shape functions. Introducing the natural coordinate system, the linear Lagrangian shape functions are given as:

$$N_1 = \frac{1}{4}(1-\xi)(1-\eta) \qquad N_2 = \frac{1}{4}(1+\xi)(1-\eta)$$
$$N_3 = \frac{1}{4}(1+\xi)(1+\eta) \qquad N_4 = \frac{1}{4}(1-\xi)(1+\eta) \tag{1}$$

Introducing the shape function matrix as:

$$[\mathbf{N}] = \begin{bmatrix} N_1 & 0 & 0 & N_2 & 0 & 0 & N_3 & 0 & 0 & N_4 & 0 & 0 \\ 0 & N_1 & 0 & 0 & N_2 & 0 & 0 & N_3 & 0 & 0 & N_4 & 0 \\ 0 & 0 & N_1 & 0 & 0 & N_2 & 0 & 0 & N_3 & 0 & 0 & N_4 \end{bmatrix} \tag{2}$$

The displacements as functions of the natural coordinates can be written in the matrix-vector form as:

$$\{\mathbf{u}^+\} = [\mathbf{N}]\{\mathbf{q}^+\}$$
$$\{\mathbf{u}^-\} = [\mathbf{N}]\{\mathbf{q}^-\} \tag{3}$$

If particle fracture occurs when the stress in the particle reaches its ultimate tensile strength, $\sigma_{p,uts}$, then setting the boundary condition at

$$\sigma_p = \sigma_{p,\,uts} \tag{4}$$

and substituting into Eq.(1) gives a relationship between the strength of the particle and the interfacial shear stress such that if

$$\sigma_{P,uts} < \frac{2\tau}{n} \tag{5}$$

Then the particle will fracture. Similarly if interfacial debonding/yielding is considered to occur when the interfacial shear stress reaches its shear strength

$$\tau = \tau_{max} \quad (6)$$

For particle/matrix interfacial fracture can be established whereby,

$$\tau_{max} < \frac{n\sigma_p}{2} \quad (7)$$

This approach suggests that the outcome of a matrix crack impinging on an embedded particle depends on the balance between the particle strength and the shear strength of the interface.

3. RESULTS AND DISCUSSION

The effect of volume fraction of titanium nitride (TiN) on the elastic moduli, E_x, E_y and G_{xy} is shown figure 4a. A slight increase in the tensile modulus was found with an increase in the volume fraction of TiN, while decrease of G_{xy} was noticed with the increase of ZrO_2 in the composites. The compressive modulus was least for the composites having 20% TiN. The major Poisson's ratio increased with increase of volume fractions of TiN (figure 4b). The reasons could be attributed the mismatches of elastic moduli and Poisson's ratios of AA6061 alloy matrix and TIN particulates. The elastic moduli of AA6061 alloy matrix and TiN particulates are, respectively, 68.9 GPa and 251 GPa. The Poisson's ratios of AA6061 alloy matrix and TiN particulates are, respectively, 0.33 and 0.25.

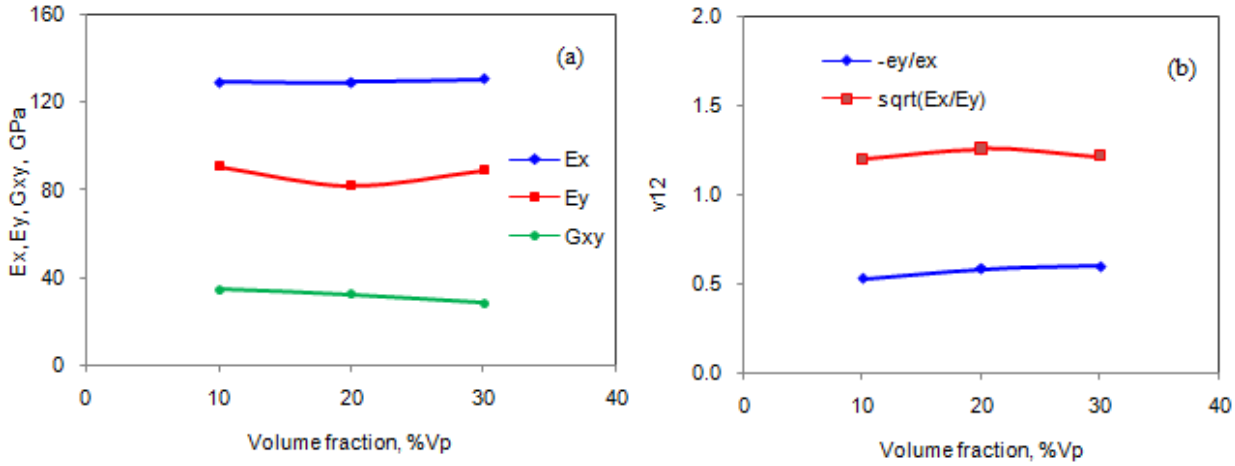

Figure 4: Effect of volume fraction on effective material properties.

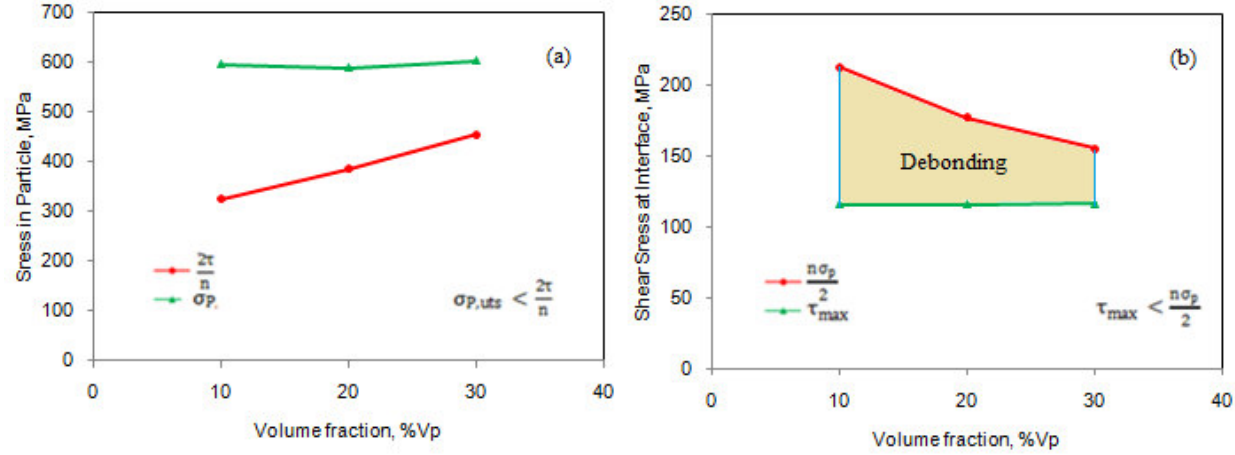

Figure 5: Fracture criteria of: (a) particulate fracture and (b) interface debonding.

The particulate fracture was not revealed in the composites as shown in figure 5a. The TiN particulate fracture was not produced as the condition $\sigma_p \leq 2\tau/n$ is not satisfied. The condition $\tau_{max} < n\sigma_p/2$ is satisfied for the occurrence of debonding in the composites including 10%, 20% and 30% TiN (figure 5b). The strain energy density increased in the AA6061 alloy matrix with an increase in the volume fraction of TiN (figure 6). The strain energy density decreased at the interface with an increase

in the volume fraction of TiN. Nevertheless, the strain energy density of TiN increased in the composites. This represents the debonding tendency at the interface between AA6061 alloy matrix and TiN nanoparticulates. The decreased strain energy density attributes to the interface debonding. The strain energy density in the TiN nanoparticulates was lower than that developed in the matrix and at the interface. The normal and tangential tractions are higher for AA6061/30%TiN composites than that for AA6061/10%TiN and AA6061/20%TiN composites (figure 7). The normal traction is highest along the loading direction leading to debonding in that direction. The interface debonding increased with an increase in the volume fraction of TiN as shown in figure 8.

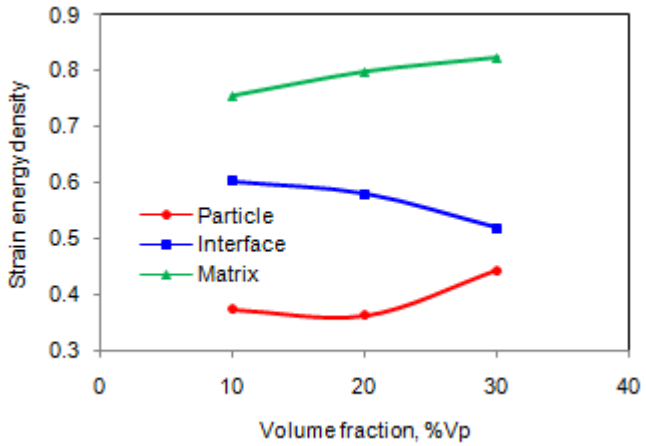

Figure 6: Effect of volume fraction on strain energy density.

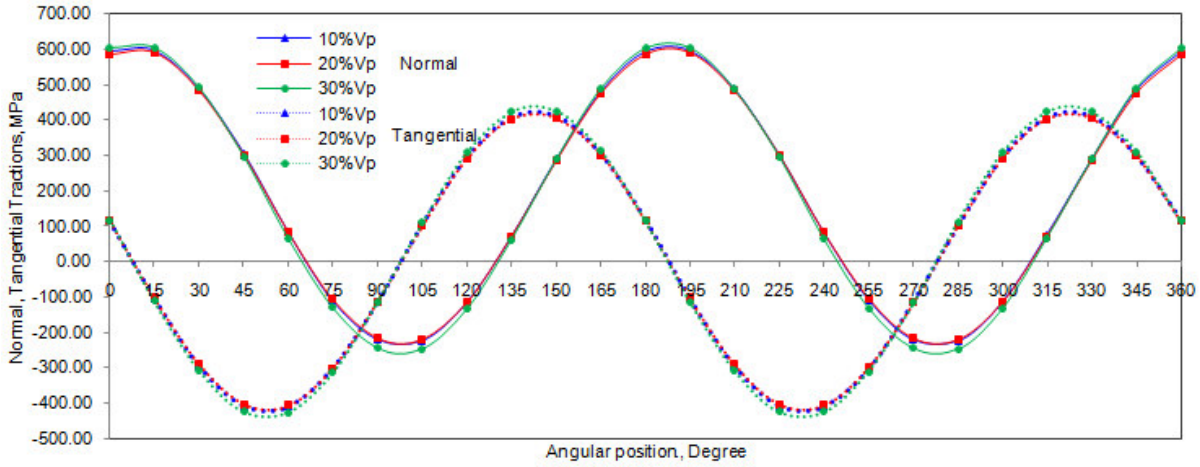

Figure 7: Normal and tangential tractions.

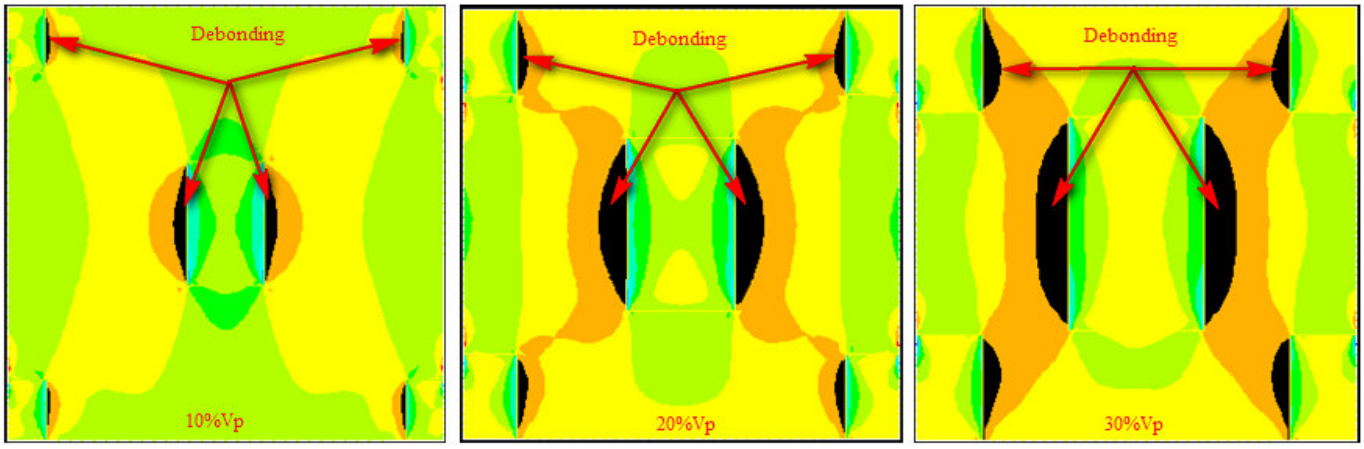

Figure 8: Results of cohesive zones obtained from finite element analysis for debonding.

4. CONCLUSION

The interface debonding occurred in the composites containing 10% , 20% and 30% volume fractions TiN.; Nanoparticulate damage had not occurred. The interface debonding increased with an increase of volume fractions of TiN in the composites.

REFERENCES

1. S. Ghosh and S. Moorthy, Particle fracture simulation in non-uniform microstructures of metal-matrix composites. Acta Mater. 46, 1998, pp.965–982.
2. G. I. Barenblatt, The Mathematical Theory of Equilibrium Cracks Formed in Brittle Fracture. Zhurnal Prikladnoy Mekhaniki I Tekhnicheskoy 1 (4), 1961.
3. S. Sundara Rajan and A. Chennakesava Reddy, Assessment of Tensile Behavior of Boron Carbide/AA2024 Alloy Metal Matrix Composites, 1st International Conference on Composite Materials and Characterization, Bangalore, March 1997, pp.160-163.
4. P. Martin Jebaraj and A. Chennakesava Reddy, Prediction of Micro-stresses and interfacial Tractions in Boron Carbide/AA6061 Alloy Metal Matrix Composites, 1st International Conference on Composite Materials and Characterization, Bangalore, March 1997, pp. 183-185.
5. B. Kotiveera Chari and A. Chennakesava Reddy, Computation of Micro-stresses and interfacial Tractions in Boron Carbide/AA7020 Alloy Metal Matrix Composites, 1st International Conference on Composite Materials and Characterization, Bangalore, March 1997, pp. 186-188.
6. P. Martin Jebaraj, A. Chennakesava Reddy, Effect of Interfacial Debonding on Stiffness of Titanium Boride/AA5050 Alloy Metal Matrix Composites, 1st National Conference on Modern Materials and Manufacturing, Pune, 19-20 December, 1997.
7. S. Sundara Rajan, A. Chennakesava Reddy, Micromechanical modeling of Titanium Boride/AA7020 Alloy Metal Matrix Composites in Finite Element Analysis using RVE Model, 1st National Conference on Modern Materials and Manufacturing , Pune, 19-20 December, 1997.
8. P. Martin Jebaraj, A. Chennakesava Reddy, Effect of Interfacial Tractions of Rectangular Titanium Boride Particulate/AA8090 Alloy Metal Matrix Composites , 1st National Conference on Modern Materials and Manufacturing , Pune, 19-20 December, 1997.
9. S. Sundara Rajan, A. Chennakesava Reddy, Cohesive Zone interfacial debonding of SiliconNitride/AA1100 Alloy Metal Matrix Composites Using Finite Element Analysis , 1st National Conference on Modern Materials and Manufacturing, Pune, 19-20 December, 1997.
10. S. Sundara Rajan, A. Chennakesava Reddy, Simulation of Micromechanics for interfacial debonding in Silicon Nitride/AA2024 Alloy Metal Matrix Composites , 1st National Conference on Modern Materials and Manufacturing, Pune, 19-20 December, 1997.
11. P. Martin Jebaraj, A. Chennakesava Reddy, Finite Element Analysis for Assessment of Dislocation and Debonding Events in Silicon Nitride/AA3003 Alloy Metal Matrix Composites, 1st National Conference on Modern Materials and Manufacturing, Pune, 19-20 December, 1997.
12. A. Chennakesava Reddy, Evaluation of Debonding and Dislocation Occurrences in Rhombus Silicon Nitride Particulate/AA4015 Alloy Metal Matrix Composites, 1st National Conference on Modern Materials and Manufacturing, Pune, India, 19-20 December, 278-282, 1997.